

pubs.acs.org/JACS Article

# Axially Chiral Cannabinoids: Design, Synthesis, and Cannabinoid Receptor Affinity

Sara E. Kearney, Anghelo J. Gangano, Daniel G. Barrus, Kyle J. Rehrauer, Terry-Elinor R. Reid, Primali V. Navaratne, Emily K. Tracy, Adrian Roitberg, Ion Ghiviriga, Christopher W. Cunningham,\* Thomas Gamage,\* and Alexander J. Grenning\*



Cite This: J. Am. Chem. Soc. 2023, 145, 13581-13591



ACCESS

Metrics & More

Article Recommendations

Supporting Information

**ABSTRACT:** The resorcinol-terpene phytocannabinoid template is a privileged scaffold for the development of diverse therapeutics targeting the endocannabinoid system. Axially chiral cannabinols (axCBNs) are unnatural cannabinols (CBNs) that bear an additional C10 substituent, which twists the cannabinol biaryl framework out of planarity creating an axis of chirality. This unique structural modification is hypothesized to enhance both the physical and biological properties of cannabinoid ligands, thus ushering in the next generation of endocannabinoid system chemical probes and cannabinoid-inspired leads for drug development. In this full report, we describe the philosophy guiding the design of axCBNs as well as several synthetic strategies for their construction. We also introduce a second class of axially chiral

$$\begin{array}{c} \text{Me} \\ \text{9} \\ \text{10} \\ \text{OH} \\ \text{C}_5\text{H}_{11} \\ \text{(-)-trans-}\Delta9\text{-} \\ \text{tetrahydrocannabinol (THC)} \\ \text{Example of the properties of the properties$$

cannabinoids inspired by cannabidiol (CBD), termed axially chiral cannabidiols (axCBDs). Finally, we provide an analysis of axially chiral cannabinoid (axCannabinoid) atropisomerism, which spans two classes (class 1 and 3 atropisomers), and provide first evidence that axCannabinoids retain—and in some cases, strengthen—affinity and functional activity at cannabinoid receptors. Together, these findings present a promising new direction for the design of novel cannabinoid ligands for drug discovery and exploration of the complex endocannabinoid system.

# INTRODUCTION

Phytocannabinoids and their synthetic analogues are prime candidates for pharmaceutical innovation in the quest for alternatives to highly addictive opioid analgesics, though they are yet to achieve Food and Drug Administration (FDA) approval for this formidable goal.<sup>1,2</sup> More generally, cannabinoid-based chemical probes and leads are essential for continued exploration of the endocannabinoid system, a complex neuro- and immunomodulating network implicated in a variety of neurodegenerative diseases as well as inflammation, metabolic disorders, and cancer. 1,3 Most phytocannabinoid research to date has focused on the natural transtetrahydrocannabinol (trans-THC) and cannabidiol (CBD) frameworks, which have led to several approved medications (Figure 1A).<sup>4-11</sup> For example, (-)-trans- $\Delta^9$ -THC is FDAapproved (Dronabinol) for the treatment of HIV/AIDSinduced anorexia<sup>12</sup> as well as chemotherapy-induced nausea and vomiting.<sup>13</sup> The approval of CBD (Epidiolex) to treat refractory childhood seizures marked the first time a cannabisderived product was approved by the FDA. 14 Synthetic cannabinoids inspired by THC have emerged due to wellestablished synthetic protocols dating back to the 1940s<sup>15</sup> via a renaissance of research over the past ~60 years. 16 Additionally,

there are numerous inspiring routes to CBD<sup>17</sup> and minor cannabinoids.<sup>18</sup> In this regard, nabilone is approved to treat chemotherapy-induced nausea and vomiting,<sup>19</sup> and ajulemic acid has reached various clinical trial phases as a treatment for systemic sclerosis, dermatomyositis, cystic fibrosis, and systemic lupus erythematosus (Figure 1B).<sup>20</sup> Beyond the THC scaffold, other frameworks for synthetic cannabinoids have appeared, including cyclohexylphenols (e.g., CP55940),<sup>21</sup> cannabidiol derivatives (e.g., KLS-13019),<sup>22</sup> cannabilactones (e.g., AM1714),<sup>23</sup> and a variety of other heterocyclic scaffolds described elsewhere.<sup>24</sup>

Recently, we proposed that axially chiral analogues of cannabinoids may serve as valuable tools and leads for cannabinoid-based drug discovery (axCannabinoids, Figure 1C).<sup>25</sup> Scaffolds of this type are attractive for the following reasons: (i) axCannabinoids are three-dimensional biased

Received: January 5, 2023 Published: June 14, 2023





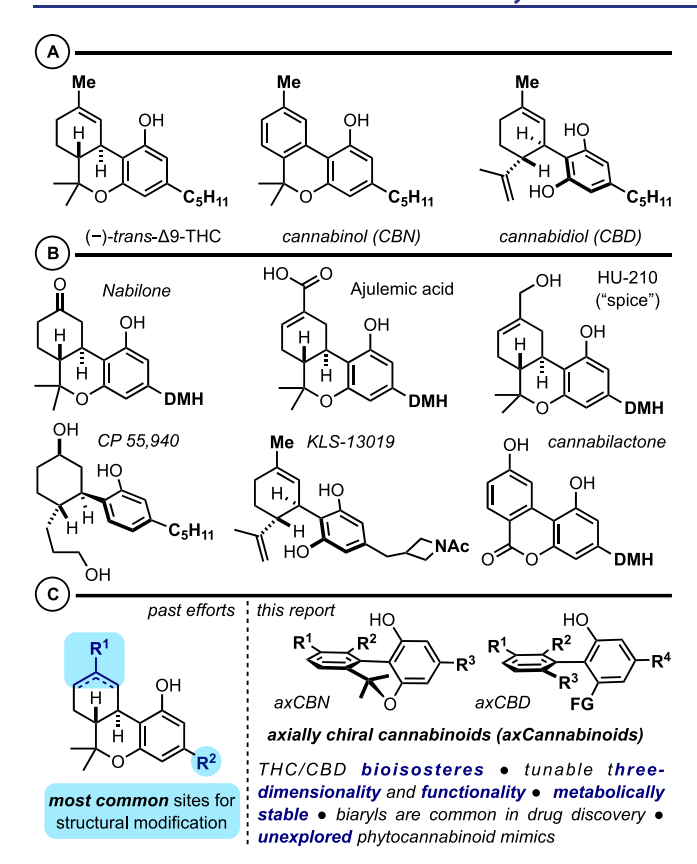


**Figure 1.** (A) Major phytocannabinoids (THC, CBN, and CBD). (B) Representative synthetic cannabinoids. (C) Past efforts and this work: *ax*Cannabinoids as bioisosteric variants with improved physical and biological properties.

ligands where additional *ortho*-substitution results in rotational and dihedral angle restrictions about the biaryl linkage. The significance of atropisomerism and the tuning of biaryl dihedral angles is a challenge and opportunity in modern drug design.  $^{26-30}$  (ii) *ax*Cannabinoids are built upon a central

biaryl framework. Biaryls are readily prepared and functionalized by numerous methods and are often metabolically stable. These features have made biaryls a common template in drug discovery campaigns. 31,32 This quality is particularly relevant to cannabinoid design as many phytocannabinoids and synthetic variants are prone to aerobic and metabolic oxidation.<sup>33</sup> (iii) Atropisomerism is unexplored with respect to cannabinoid ligands, providing potentially rich grounds for discovery and innovation. This hypothesis that structural modification of (synthetic) phytocannabinoids to axCannabinoids can impact both physical/biological properties and retrosynthesis/forward synthesis logic is strongly aligned with a recent call from Shenvi et al. for "creative editing of natural products" as an "invitation for [chemical and biological] discovery". 34 In this report, we describe our initial efforts to establish axCannabinoids as valuable lead molecules with high affinity for cannabinoid receptors. This includes synthetic strategies for accessing axially chiral cannabinols (axCBNs), introduction to and synthesis of axially chiral cannabidiols (axCBDs), and affinity studies for select axCannabinoids at the cannabinoid receptors (hCB<sub>1</sub>R and hCB<sub>2</sub>R).

### RESULTS AND DISCUSSION

**Synthetic Methods toward Axially Chiral Cannabinols** (axCBNs). We previously reported a scalable, first-generation synthesis of "parent" axially chiral cannabinol (axCBN), the C9-to-C10 methyl-transposed isomer of cannabinol (CBN) (Figure 2A). By design, this transposition results in significant topological changes to the cannabinoid architecture: the ground-state biaryl dihedral angle increases from 19° in CBN to 38° in axCBN. CBNs are relatively planar ( $\theta = 19^{\circ}$ ) with little barrier to inversion, whereas axCBNs have increased three dimensionality (( $\theta = 38^{\circ}$ ) and barriers to atropisomersim ranging from 14 to 17 kcal/mol (class 1 atropisomerisim). Retrosynthetically, we envisaged access to axCBN via an intramolecular Diels-Alder approach to biaryls (DAB).  $^{35-37}$  This revealed dimethylpropargyl chloride 1, allylcyanide 2, and the olivetol derivative 3 as potential

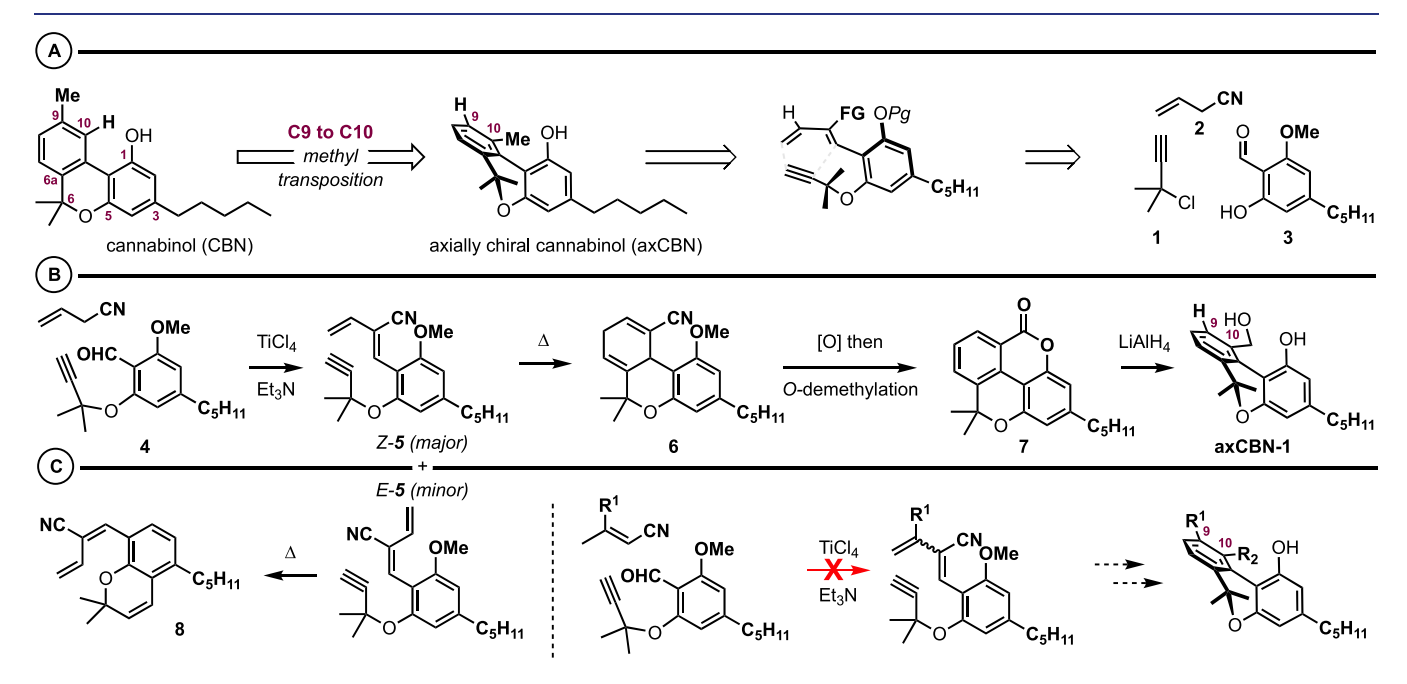
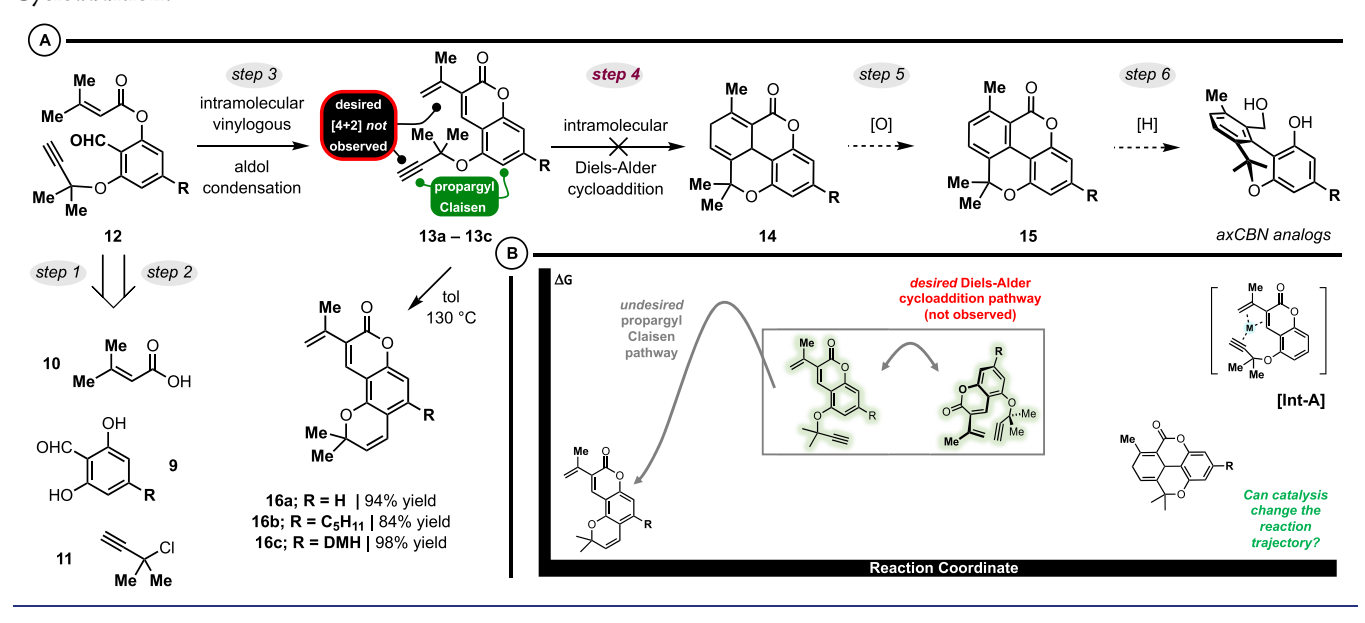
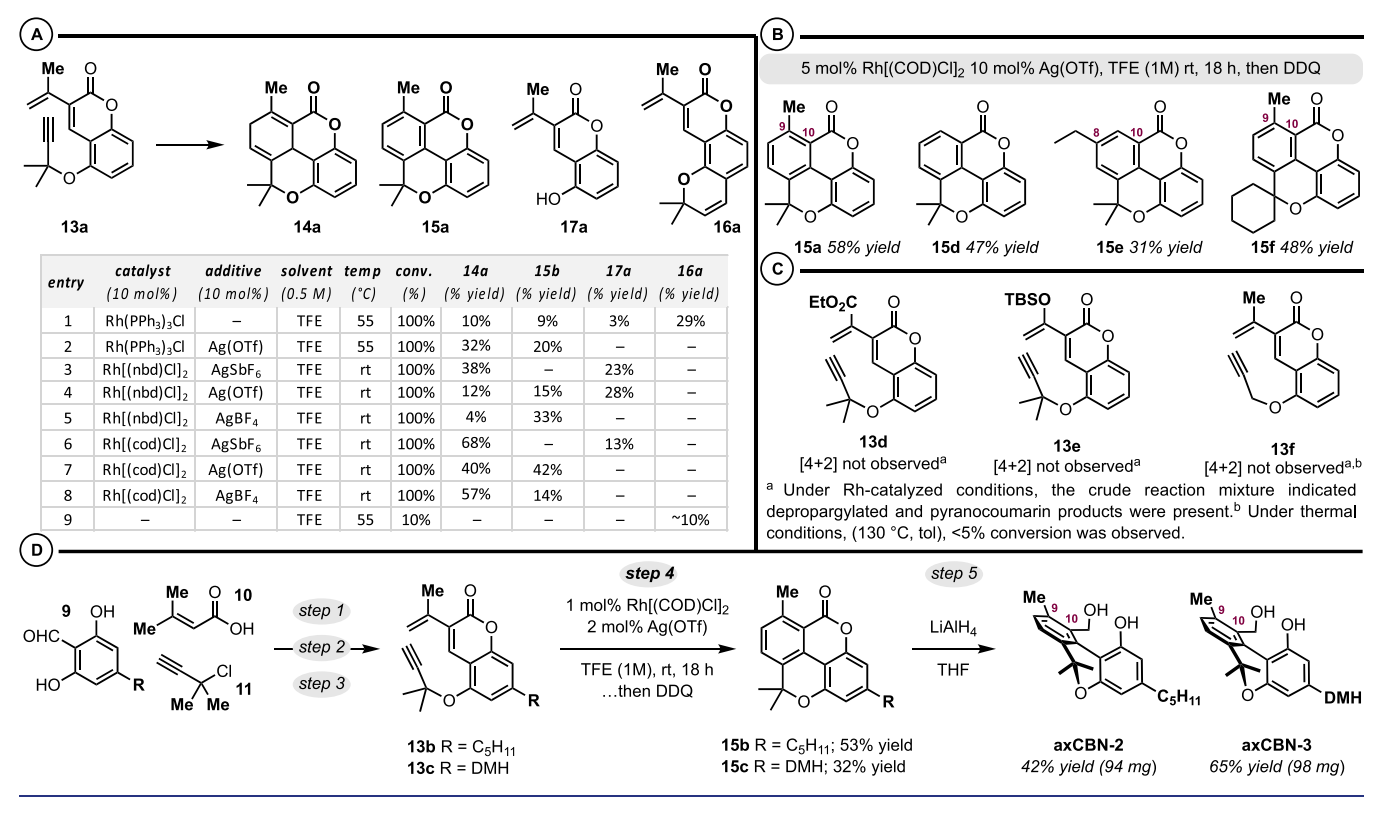


Figure 2. axCBN retrosynthesis (A), forward synthesis (B), and representative synthetic shortcomings (C).

Scheme 1. (A): Second-Generation Strategy Capable of Achieving C9 and C10 Disubstitution Is Challenged by a Competitive Propargyl Claisen Rearrangement. (B): Can the Innate [3,3] Reactivity Be Overturned in Favor of Dearomative [4+2] Cycloaddition?



Scheme 2. Optimization (A), Scope (B), and Limitations (C) of Rh-Catalyzed Dearomative [4+2] Cycloaddition. (D) Synthesis of axCBN-2 and axCBN-3



starting materials. A successful route to axCBN and other C10-substituted analogues was achieved through a key biaryllactone intermediate 7 (Figure 2B). This advanced scaffold was prepared via Cu-catalyzed dimethylpropargylation between 1 and 3 (yielding 4), TiCl<sub>4</sub>/Et<sub>3</sub>N-promoted condensation between 4 and allylcyanide 2 (yielding an inseparable mixture of E-5 and Z-5), intramolecular Diels-Alder cycloaddition (yielding 6), DDQ oxidation, and demethylative Pinner reaction (yielding 7). axCBN-1 was prepared via LiAlH<sub>4</sub>

reduction (Figure 2B) and "parent" axCBN was prepared in two additional steps.

While this initial synthetic strategy provided ample amounts of parent axCBN and axCBN-1 over a reasonably efficient synthetic sequence (6–8 steps from 1, 2, and 3), it is not without shortcomings. Synthetic challenges include a non-selective vinylogous aldol condensation that produces an inseparable mixture of E-5 and Z-5, and only the Z isomer reacts as desired in the subsequent step. As shown in Figure

2C, the *E*-5 isomer undergoes a propargyl Claisen rearrangement to benzochromene 8. More significantly, the key  $TiCl_4$ / $Et_3N$ -promoted condensation was unsuccessful with substituted crotonitriles (R  $\neq$  H), limiting the modularity of the synthetic route with respect to C9 substitution (Figure 2C).

The issues we encountered during our initial studies (Figure 2C) prompted us to explore an alternative protocol that would be capable of accessing axCBNs bearing both C9 and C10 substitution, as we hypothesized that the most active axCBN analogues would have substituents at both positions. Simple transposition of the C9 methyl group to the C10 position generates a "methyl void" on the parent scaffold, and methyl groups are known to have significant impact on drug properties (the "magic methyl effect"). 38,39 Consequently, deletion of the C9 methyl substituent may negatively impact the affinity and efficacy at cannabinoid receptors. 38 Thus, we aimed to develop a synthetic route capable of facilitating C9-methylation and C10 functionalization, as well as variation at other positions. In this regard, we envisioned access to axCBN analogues from 12 by a sequential intramolecular aldol condensation/Diels-Alder cycloaddition yielding the advanced tetracyclic intermediate 14 (Scheme 1A). Upon cyclohexadiene oxidation and biaryl lactone ring opening, axCBN analogues would be unveiled. We postulated that the key scaffold 12 could be prepared simply from the requisite olivetol-aldehyde 9, 3,3-dimethylacrylic acid 10, and dimethylpropargyl chloride 1, with known literature procedures for preparing aryl dimethylpropargyl ethers 40-42 and divinylcoumarins serving as inspiration.<sup>43</sup>

At the outset of our studies, we successfully prepared model Diels-Alder precursors 13a-13c by the proposed Cu-catalyzed dimethylpropargyl ether synthesis, phenol acylation with 3,3dimethylacrylic acid 10, and intramolecular vinylogous aldol condensation (Scheme 1A). At this point, we realized that the desired thermal [4+2] transformation would be more challenging than we initially anticipated: under thermal conditions, these substrates exclusively react via propargyl Claisen rearrangement to yield pyranocoumarins. 42,45 It became apparent that a critical Curtin-Hammett kinetics challenge exists in which the desired product 14 is neither thermodynamically nor kinetically favored over the propargyl Claisen rearrangement (Scheme 1B). Recall from Figure 2 that the Z-cyano-1,3-diene underwent favorable [4+2] cycloaddition over propargyl Claisen rearrangement. While 13 has the correct 1,3-diene geometry, the kinetics and thermodynamics of the desired [4+2] cycloaddition are less favorable due to the aromaticity of the coumarin (which must be broken during the Diels-Alder reaction). 43,46,47 Thus, to achieve the desired transformation, reversal of the innate Curtin-Hammett controlled reactivity is necessary. Toward this goal, we envisioned that a transition-metal catalyst could template the diene and dienophile (via intermediate-A (Int-A); Scheme 1B), resulting in an altered kinetic profile and mechanism favoring formation of the coumarin-dearomatized [4+2] product (Figure 2). While there are many examples of metalcatalyzed [4+2] cycloisomerization, 48-55 vinylcoumarins as dienes, dearomatization, and Curtin-Hammett kinetics challenges are novel to this research area.

To achieve the desired [4+2] reactivity, rhodium(I) catalysis was examined (Scheme 2A). S3-S5 Using Wilkinson's catalyst ((PPh<sub>3</sub>)<sub>3</sub>RhCl) in trifluoroethanol (entry 1), we observed a complex mixture of products that notably contained the desired [4+2] cycloadduct 14a and its oxidation product, biaryl 15a. Also observed were the depropargylated product 17a and

the propargyl Claisen rearrangement product 16a. The addition of catalytic Ag(OTf) improved the result to 32% yield 14a and 20% yield 15a (entry 2). Catalytic [Rh(NBD)-Cl]2/Ag(I) additives performed comparably to Wilkson's catalyst/Ag(OTf) (entries 3-5 versus entry 2). The best results were achieved with catalytic [Rh(COD)Cl]<sub>2</sub>/Ag(I) salts in trifluoroethanol (entries 6-8) where combined 68-82% yields of 14a and 15a were obtained. Notably, the reaction performed similarly well on the 1 mmol scale (see the Supporting Information). As a control, we examined the reaction catalyst-free in trifluoroethanol (entry 9), confirming the essential impact of the catalyst. We briefly examined the scope of the transformation targeting the tetracyclic scaffolds 15a-15f (Scheme 2B,C). Products 15 were directly prepared from 13 via a one-pot, two-step Rh(I)-catalyzed [4+2] cycloaddition followed by in situ DDQ oxidation of the intermediate 1,4-cyclohexadiene. 56 Products 15d and 15e represent variations in the diene component. Unsubstituted (15d) and ethyl-substituted (15e) dienes were reasonably tolerated. In contrast, modifications to the diene electronics resulted in little to no sign of the desired products (Scheme 2C). For example, ester substrate 13d and the silyl-enol ether diene 13e were not competent Diels-Alder substrates. With respect to the propargylic substitution on the dienophile, a cyclohexyl group was tolerated yielding 15f. However, in the absence of substitution, the transformation did not occur (Scheme 2C, 13f).

The scope studies related to the Rh(I)-catalyzed [4+2] cycloaddition suggest that a variety of C8/C10 (15e) and C9/C10 (15a and 15f) disubstituted *ax*CBNs can be accessed. Along these lines, coumarins 13b and 13c bearing the common cannabinoid aliphatic chains (pentyl and dimethylheptyl (DMH), respectively) on the resorcinol-portion of the scaffold were prepared (Scheme 2D). Gratifyingly, the Rh(I)-catalyzed [4+2] cycloaddition/oxidation sequence yielded the desired pyrano-biaryllactones 15b and 15c. LiAlH<sub>4</sub> reduction furnished the targeted *ax*CBN analogues, *ax*CBN-2 and *ax*CBN-3.

Synthetic Methods toward Axially Chiral Cannabidiols (axCBDs). During our studies related to the firstgeneration route to axCBNs (Figure 2), specifically, the attempted demethylation to free the phenol on 6, we encountered a transformation that converted the Diels-Alder adduct 6a into the biaryl 18a with concomitant pyran ring cleavage (Scheme 3). We surmised that this transformation occurred by an "E1<sub>cb</sub> aromatization." In this process, the nitrile group directs deprotonation yielding int-B, which is poised for pyran ring-cleavage to phenoxide int-C. In situ or upon acidic work up, int-C undergoes a thermodynamically favorable isomerization from the nonaromatic isotoluene to the biaryl product 18. This was an interesting outcome as it resulted in an axially chiral biaryl by a unique method, and the structure is reminiscent of the theoretical "parent" axially chiral cannabidiol (axCBD). Regarding the method, the Diels-Alder reaction between dienes and alkynes to yield arenes usually relies on oxidation of the intermediate 1,4-cyclohexadiene<sup>57</sup> or elimination of an endocyclic leaving group. 58,59 Thus, this represents a unique strategy for targeting substituted and functionalized arenes. With respect to CBD, axCBD is formulated in analogy to the relationship between THC and axCBN: the cyclohexene ring of the parent natural product is formally oxidized to the arene, and the methyl group is transposed from the C9 to the C10 position, thus resulting in axially chiral cannabidiols. This term should be considered

Scheme 3. (A) Observation of an E1<sub>cb</sub> Elimination Reaction Yielding a Biaryl Reminiscent of Parent axCBD. (B) Cannabidiol (CBD) and Axially Chiral Cannabidiol (axCBD)

A CNOMe 12 equiv. NaSEt DMF, 120 °C 44% yield (
$$\pm$$
) 18a ( $\pm$ ) 18a

loosely as parent axCBD is prochiral rather than chiral, but it bears an orthogonal, conformationally restricted biaryl linkage and thus is three-dimensional. That said, many axCBD analogues have the potential to be axially chiral biaryls.

Intrigued by the initial result and the potential to mimic the structure of cannabidiol (CBD) with axially chiral analogues, we designed a model substrate to optimize the E1<sub>cb</sub> aromatization sequence for targeting axCBDs (Scheme 4). The key substrates (6a-6i) were prepared by the same synthetic sequence outlined in Figure 2: (i) TiCl<sub>4</sub>/Et<sub>3</sub>Nmediated aldol condensation between allyl cyanide and the requisite O-dimethylpropargylsalicylaldehyde then (ii) intra-

Scheme 4. (A) Biaryl Synthesis via E1<sub>cb</sub> Aromatization: Scalability and Scope Studies. (B) Synthesis of axCBD-1 and ax-CBD-2 Utilizing E1<sub>cb</sub> Aromatization

18i 44% vield: 219 mas

6iR = DMH

molecular Diels-Alder cycloaddition. It was found that various bases could instigate the E1<sub>cb</sub> aromatization, but LiHMDS was optimal (see the Supporting Information for select optimization reactions). This reaction can be performed on the gram scale, and a variety of unique o-benzonitrile-o'-phenol biaryls were prepared in good yields under the optimized protocol. Notably, halogen functional handles are tolerated at every position about the phenol (18c-18g), and an o-benzonitrileo'-naphthol biaryl 18h is accessible. With the goal of applying this method to the synthesis of axCBD analogues, Diels-Alder adducts 6a and 6i were accessed on the 0.5-1 g scale. Under the standard E1<sub>cb</sub> aromatization conditions, we prepared the advanced axially chiral biaryl intermediates 18a and 18i in good yields (54 and 44%, respectively). Nitrile reduction to the alcohol was achieved via sequential addition of DIBALH and NaBH<sub>4</sub> yielding axCBD-1 (R = pentyl) and axCBD-2 (R = dimethylheptyl (DMH)).

Atropisomerism of Axially Chiral Cannabinoids. Axially chiral cannabinols (axCBNs) and cannabidiols (axCBDs) differ from their respective natural product counterparts, THC and CBD in two main ways: (1) by oxidation of the natural cyclohexene to a benzene ring and (2) by C9 to C10 methyl transposition. These structural modifications result in nonplanar biaryl scaffolds, rotational restrictions about the biaryl linkage, and tunable three dimensionality: variation of the ortho-substituents and ring types directly influences the dihedral angles and barriers to atropisomerism. For example, the barrier to atropisomerism for axCBN-2 and its bis-acetate, axCBN-4, was found by VT-NMR to be 14 and 17 kcal/mol, respectively (Scheme 5).

Scheme 5. (A) axCBNs Display "type 1" Atropisomerism. (B) axCBDs Display "type 3" Atropisomerism.

Regarding axCBDs, VT-NMR experiments indicated that the biaryl linkage was conformationally stable: no coalescence of the enantiotopic signals was observed up to 95 °C in toluene-D<sub>8</sub>. These studies revealed that we have synthesized two classes of axially chiral cannabinoid thus far: axCBNs are class 1 atropisomers while axCBDs are class 3 atropisomers. 26-30 As

rac-axCBD-2; 28% yield

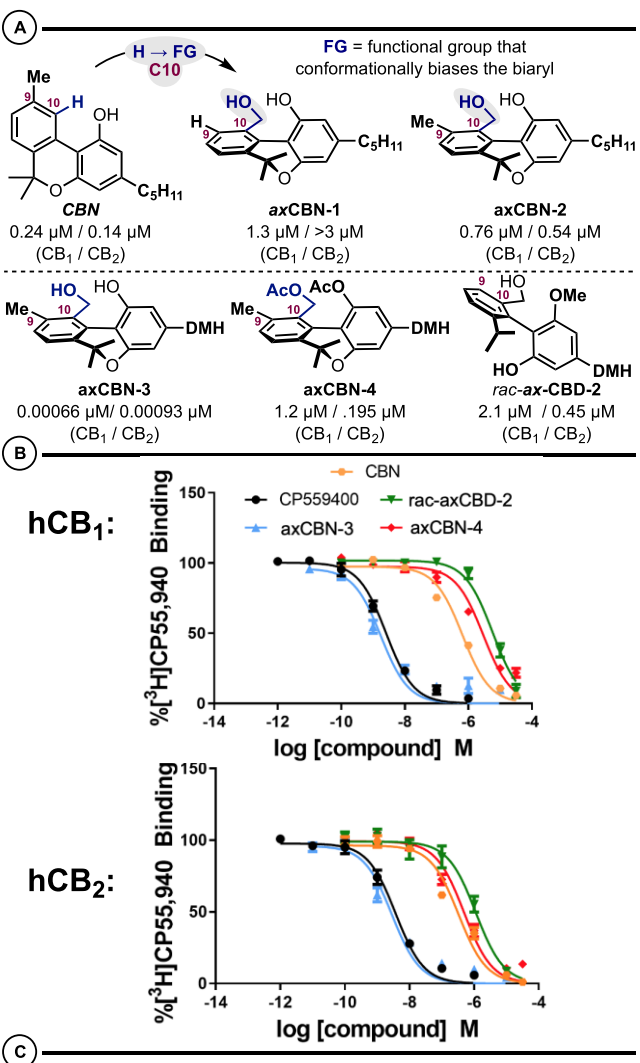
such, axCBNs can be treated as achiral molecules due to the rapid interconversion of the individual atropisomers, though they would presumably bind their targets in chiral non-racemic configurations (vide infra). Conversely, axCBDs are configurationally stable and the individual atropisomers could have different binding affinities for their targets (vide infra).

Molecular Pharmacology of Axial Chiral Cannabinoids at Cannabinoid Receptors. We have examined a small series of axCannabinoids for binding affinity and functional activity at human cannabinoid receptors (hCB<sub>1</sub>R and hCB<sub>2</sub>R) (Schemes 6 and 7). From this initial series, several compounds emerged with desirable pharmacology relative to the relevant parent phytocannabinoid in terms of affinity and selectivity. axCBN-3 exhibited sub-nanomolar affinity for both receptors, approximately 360-fold higher than CBN at hCB<sub>1</sub>R and 134-fold higher at hCB<sub>2</sub>R.<sup>60</sup> When compared to the dimethylheptyl derivative of CBN (CBN-DMH) reported by Rhee and co-workers, <sup>60,61</sup> axCBN-3 has approximately 5-10fold higher affinity. This suggests that the addition of the C-10 group, which biases the biaryl to a nonplanar configuration, confers additional beneficial interactions with hCB1R and hCB<sub>2</sub>R that result in higher affinity. Notably, axCBN-3 demonstrated affinity similar to that of the positive control, CP55940, at both receptors. 58 Additionally, axCBD-2 and axCBN-4 exhibited increased selectivity for hCB2R, 4.8- and 6.2-fold, respectively.

Importantly, these compounds maintained functional activity as determined by stimulation of [35S]GTPγS binding, an assay of native G protein activation (Supplementary Tables 4 and 5). axCBN-3 exhibited an 8-fold greater potency to stimulate [35S]GTPγS binding at hCB<sub>2</sub>R than at hCB<sub>1</sub>R while exhibiting increased efficacy over CBN. axCBN-4 also maintained agonist activity at hCB2R. Notably, axCBD-2 exhibited 7.4-fold greater potency in [35S]GTPγS binding. Further, axCBD-2 exhibited agonism at hCB2R in the TRUPATH assay of  $G\alpha i 1\beta 3\gamma 9$  protein activation (Supplementary Tables 6 and 7), but not at hCB<sub>1</sub>R at concentrations up to 31.6  $\mu$ M (Scheme 6D), suggesting a potential route for development of selective hCB2R agonists. This functional activity diverges from that of the parent CBD which exhibits no efficacy at either cannabinoid receptor in either of these assays (data not shown). Interestingly, in contrast to CBN [F(2, 64) = 1.21, p = 0.305], axCBN-3 [F(2, 91) = 42.7, p <0.0001] exhibited distinct affinities for two binding sites following an extra sum-of-squares F test for one site versus two site binding models (Scheme 7). The higher affinity binding may reflect selection for the active conformation, which is also supported by the higher efficacy of axCBN-3 in [35S]GTPγS binding (Supplementary Tables 4 and 5). Further, because axCBN-3 is a class 1 atropisomer, it exists as two enantiomeric conformers rapidly equilibrating, each of which may have unique affinities for different conformations and give rise to multiphasic binding curves as depicted in Scheme 6. Thus, these compounds may exhibit particularly unique pharmacology in terms of the receptor populations they could stabilize to give rise to unique signaling profiles.

Racemic axCBD-2 is configurationally stable (Scheme 5) and demonstrably active at cannabinoid receptors and selective for hCB<sub>2</sub>R (Scheme 6). To understand the impact of axial chirality on cannabinoid receptor affinity, the enantiomers were separated and subject to further molecular pharmacology studies (Scheme 8). Regarding the separation, this was achieved using Supercritical Fluid Chromatography (SFC) as

Scheme 6. (A) axCannabinoid Summary. (B) Displacement of [3H]CP55940 Binding. (C) axCannabinoid Binding Affinity at Cannabinoid Receptors. (D) TRUPATH Gαi Activation

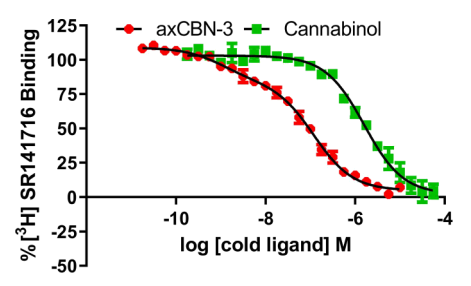


	hCB₁R		hCB₂F	hCB₂R		
compound	pK <sub>i</sub> ± SEM	K <sub>i</sub> (nM)	pK <sub>i</sub> ± SEM	K <sub>i</sub> (nM)	CB <sub>1</sub> /CB <sub>2</sub>	
CP55,940	9.03 ± 0.0292	0.933	8.86 ± 0.107	1.38	0.7	
CBN	6.62 ± 0.0627	240	6.86 ± 0.0370	138	1.7	
CBD	5.48 ± 0.0605	3310	5.85 ± 0.0374	1410	2.3	
∆8-THC	7.81 ± 0.0963	15.4	7.68 ± 0.107	20.7	0.7	
∆9-THC	7.61 ± 0.0459	24.5	7.53 ± 0.133	29.8	0.8	
ax CBD-2	5.67 ± 0.0821	2140	6.35 ± 0.0755	447	4.8	
ax CBN-3	9.18 ± 0.0794	0.661	9.03 ± 0.141	0.933	0.7	
ax CBN-4	5.92 ± 0.125	1200	6.71 ± 0.122	195	6.2	

compound	hC	B₁R	hC	hCB₂R		
compound	pEC <sub>50</sub>	E <sub>max</sub>	pEC <sub>50</sub>	E <sub>max</sub>		
CP55,940	$9.09 \pm 0.476$	0.0913 ± 0.0173	9.17 ± 0.108	0.121 ± 0.0298		
ax CBN-3	$7.58 \pm 0.763$	0.0807 ± 0.0141	8.46 ± 0.182	0.120 ± 0.0296		
ax CBN-4	5.15 ± 0.954	0.175 ± 0.0832	6.75 ± 0.397	0.120 ± 0.0294		
ax CBD-2	NA	NA	7.54 ± 0.381	0.0839 ± 0.0176		

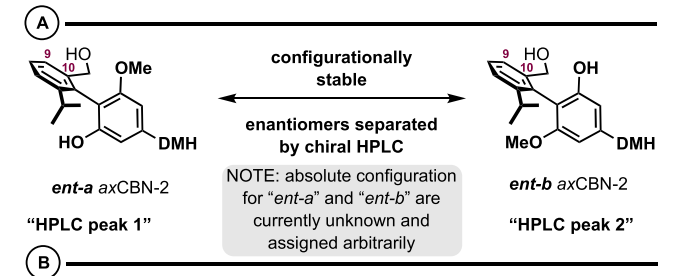
Values reflect mean ± SEM of at least N = 3 experiments performed in triplicate. NA = no observable agonism at concentrations up to 31.6 μM

described in the Supporting Information. By this method, we were able to access single enantiomers of axCBD2 (ent-a axCBD-2 and ent-b axCBD-2), but the absolute stereoScheme 7. axCBN-3 Exhibits Two Distinct Affinities at  $hCB_1R$  (pKi<sub>Hi</sub> = 9.4, pKi<sub>Lo</sub> = 7.3), Unlike CBN (pKi = 6.2), Suggesting High Affinity Binding to the Active Conformation<sup>6</sup>



<sup>a</sup>Data are mean  $\pm$  SEM of N = 3-4 experiments performed in triplicate.

Scheme 8. Effect of Absolute Configuration on Affinity and Activity at Cannabinoid Receptors. (A) Preparation of Single Enantiomers. (B) Affinity Assays. (C) GTPγS. (D) TRUPATH G $\alpha$ i1 Activation



aamnaund	hCB₁R		hCB₂R		selectivity
compound	$pK_i \pm SEM$	K <sub>i</sub> (nM)	pK <sub>i</sub> ± SEM	Ki (nM)	CB <sub>1</sub> /CB <sub>2</sub>
CP55,940	8.90 ± 0.0786	1.27	9.07 ± 0.115	0.85	0.7
rac-ax CBD-2	5.67 ± 0.0821	2140	6.35 ± 0.0755	447	4.8
ent-a-ax CBD-2	5.54 ± 0.0781 <sup>a</sup>	2900	6.19 ± 0.0437 <sup>a</sup>	642	4.5
ent-b-ax CBD-2	5.31 ± 0.0561 <sup>a</sup>	4840	6.56 ± 0.0665 <sup>a,b</sup>	278	17.4

<sup>a</sup> p < 0.0001 vs. CP55,940 <sup>b</sup> p < 0.01 vs *ent-a* 

(c)

(D).

compound	hCB <sub>1</sub> R			hCB₂R		
compound	$pEC_{50}$	EC <sub>50</sub>	$E_{max}$	pEC <sub>50</sub>	EC <sub>50</sub>	E <sub>max</sub>
CP55,940	$8.37 \pm 0.04$	4.27 nM	346 ± 29.7	9.60 ± 0.124	0.25 nM	122 ± 8.94
ent-a-ax CBD-2	ND	ND	ND	6.72 ± 0.330 <sup>b</sup>	189 nM	56.3 ± 8.51 <sup>b</sup>
ent-b-ax CBD-2	ND	ND	ND	6.74 ± 0.284°	183 nM	87.5 ± 4.24 <sup>a</sup>

 $^{\rm a}$  p < 0.05 vs. CP55,940  $^{\rm b}$  p < 0.001 vs. CP55,940  $^{\rm c}$  p < 0.0001 vs. CP55,940

compound	hC	B₂R
	pEC <sub>50</sub>	E <sub>max</sub>
CP55,940	9.25 ± 0.0989	0.0991 ± 0.00848
rac-ax CBD-2	6.47 ± 0.157 <sup>a</sup>	0.0852 ± 0.0166
ent-a-ax CBD-2	$5.96 \pm 0.156^{a}$	0.0906 ± 0.00843
ent-b-ax CBD-2	6.34 ± 0.155 <sup>a</sup>	0.0996 ± 0.0100

<sup>&</sup>lt;sup>a</sup> p < 0.0001 vs. CP55,940

Values reflect mean ± SEM of at least N = 3 experiments performed in duplicate or triplicate. ND = Not determined

chemistry of the atropisomers was not determined for this study (Scheme 8A). With respect to pharmacology, ent-b axCBD-2 exhibited 2.3-fold greater affinity at hCB2R compared to ent-a axCBD-2 in receptor binding, 278 and 642 nM, respectively (Scheme 8B). However, there was no significant difference in affinity at hCB<sub>1</sub>R (Scheme 8A, footnote a). In the case of ent-b axCBD-2, this translates to

an up to 17-fold selectivity for hCB<sub>2</sub>R, which is directly linked to the axial chirality element of the cannabinoid analogues. Both enantiomers exhibited similar potency at stimulating [35S]GTPγS binding in hCB<sub>2</sub>R expressing HEK293 cell membranes, but there was no detectable stimulation in hCB<sub>1</sub>R expressing HEK293 cell membranes (Scheme 8C). *ent-b* axCBD-2 trended to exhibit higher efficacy at stimulating [35S]GTP $\gamma$ S binding versus *ent-a* axCBD-2 (P = 0.06) in hCB<sub>1</sub>R membranes. In TRUPATH, the enantiomers stimulated activation of  $G\alpha i 1\beta 3\gamma 9$  proteins with similar potency and efficacy (Scheme 8D). The enantiomers exhibited apparent inverse agonism with low potency in HEK293 cells expressing hCB<sub>1</sub>R (data not shown).

Together, these data showcase that axCBNs and axCBDs can mimic—or even surpass—the activity of phyto- and synthetic cannabinoids at cannabinoid receptors. These analogues occupy a unique conformational chemical space (ground-state three-dimensional structures), which may impact affinity and selectivity for biological targets (cannabinoid receptors and beyond). Furthermore, the conformational restrictions unique to axCannabinoids may also provide improved physical, drug-like properties including metabolic and aerobic stability and solubility. Finally, in cases where the axCannabinoids are configurationally stable (axCBDs, namely), there is a clear indication that the absolute configuration will have significant impact on the overall affinity and activity at cannabinoid receptors. In this regard, we have found an axial chirality-dependent activity of ent-b axCBD-2 at

Molecular Modeling of axCannabinoids at Cannabi**noid Receptors.** We used induced-fit docking (Glide-XP, Schrödinger, Inc.) to predict how axCannabinoids axCBN-3 and rac-axCBD-2 engage hCB<sub>1</sub>R and hCB<sub>2</sub>R.<sup>62</sup> The Glide-XP docking scoring function is an approximated binding affinity that is used to rank predicted poses of a ligand as a result of its interaction with a target: axCBN-3 had an appreciable score with hCB<sub>1</sub>R (XPgscore -13.285 kcal/mol) and hCB<sub>2</sub>R (XPgscore -13.711 kcal/mol), and rac-axCBD-2 had lower predicted affinity in hCB<sub>1</sub>R (XPgscore -12.488 kcal/mol) compared to hCB<sub>2</sub>R (XPgscore -13.117 kcal/mol). In each case, the dimethylheptyl tails of the axCannabinoids occupy the same narrow hydrophobic channel between transmembrane helix (TMH) 3, 5, and 6 as the cocrystalized ligand (Figure 3). Hydrophobic aromatic interactions with Phe268 (hCB<sub>1</sub>R) and Phe87, Phe94 and Phe183 (hCB<sub>2</sub>R) are also observed. Canonical structure—activity relationships of classical cannabinoids indicate that a free phenol at position 1 is generally required for hCB<sub>1</sub>R and hCB<sub>2</sub>R binding.<sup>58</sup> For axCBN-3, this group is not predicted to form beneficial interactions with hCB<sub>1</sub>R but is predicted to donate a hydrogen bond to Ser285 in hCB<sub>2</sub>R; the equivalent Ser383 in hCB<sub>1</sub>R does donate a hydrogen bond to the oxygen in the pyran ring. The 10-hydroxymethyl group of axCBN-3 is predicted to form an intramolecular hydrogen bond (IMHB) with the nearby 1phenol. This may contribute to target binding by overall lowering the hydrophilicity of this region, allowing this group to occupy an otherwise hydrophobic portion of the binding site. The predicted binding pose of rac-axCBD-2 differs from that of axCBN-3 due to the larger dihedral angle connecting the two phenyl rings (ranging from -27.9° to 29.2° for axCBN-3 and  $-75.1^{\circ}$  to  $-75.3^{\circ}$  for rac-axCBD-2 when docked in hCB<sub>1</sub>R and hCB<sub>2</sub>R, respectively; see Figures S3-S6 in the Supporting Information). Within hCB<sub>1</sub>R, the 6-propyl

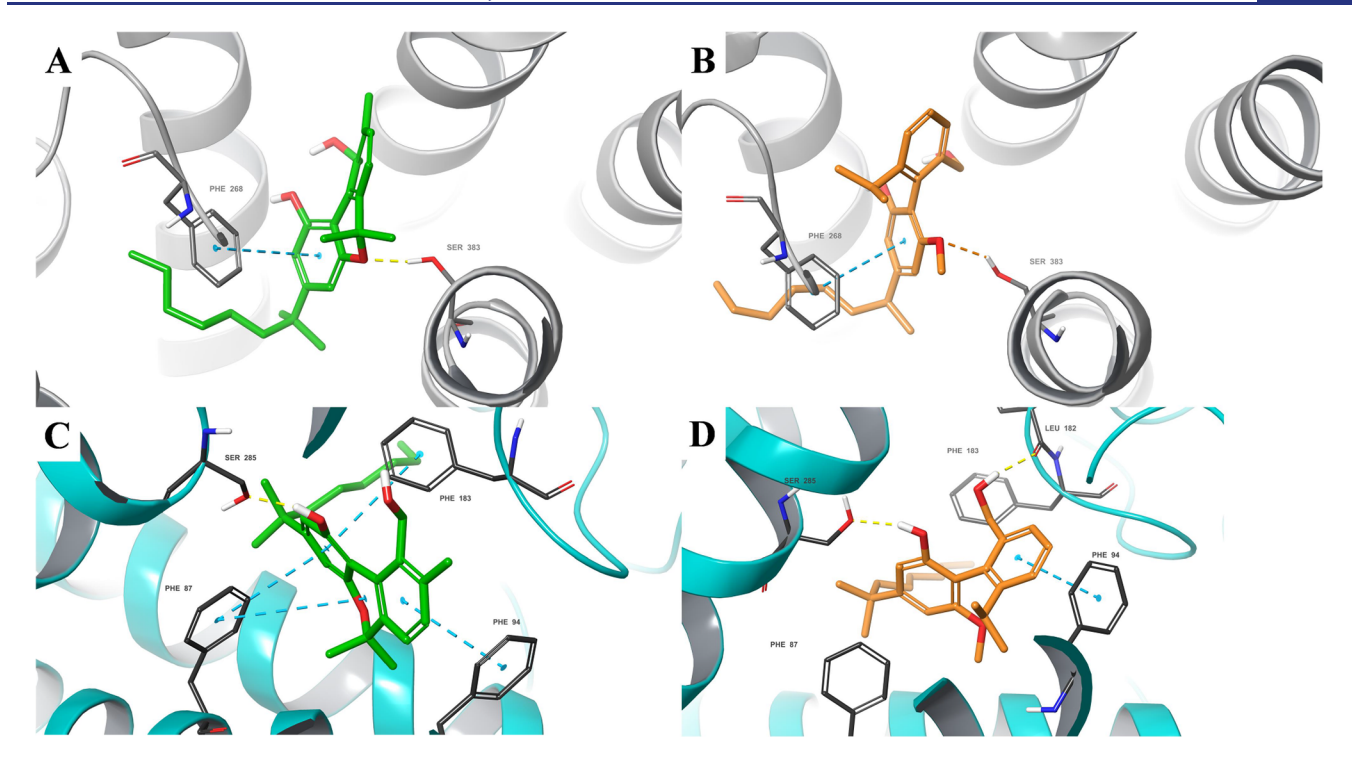


Figure 3. Results from automated docking. axCBN-3 (green) docked within hCB<sub>1</sub>R (gray) (A) and hCB<sub>2</sub>R (cyan) (C), rac-axCBD-2 (orange) docked within hCB<sub>1</sub>R (B) and hCB<sub>2</sub>R (D). For docking scores, please see the text.

substituent points toward Phe268, while the 10-hydroxymethyl group occupies a narrow lipophilic region below the plane of aryl ring A. Multiple steric clashes contribute to a lower Glide score, including a clash with Ser383. Within hCB<sub>2</sub>R, however, the 10-hydroxymethyl group is able to donate a hydrogen bond to the backbone carbonyl of Leu182, and the phenol forms a beneficial hydrogen bond with Ser285. The presence of these additional beneficial binding interactions may explain the observation that rac-axCBN-2 is a selective hCB2R agonist. This may also explain the difference in binding affinities between the two resolved atropisomers: the opposite atropisomer would be unable to form a hydrogen bond with Ser285 and would therefore be expected to have lower affinity for hCB<sub>2</sub>R than the atropisomer docked in Figure 3. More studies are needed to test this hypothesis and determine how structural modification of this novel hit influences target binding and intrinsic activity.

# CONCLUSIONS AND OUTLOOK

We have conceptualized and validated axCannabinoids as novel leads for cannabinoid-inspired drug discovery. We hypothesize that axCannabinoids will be uniquely valuable scaffolds due to their three-dimensionality and stability imparted by the central axially chiral biaryl framework. Through the development of various de novo synthetic routes and collaborative biological analysis at cannabinoid receptors (hCB<sub>1</sub>R/hCB<sub>2</sub>R), we have achieved a preliminary understanding of axCannabinoid structure-activity relationships. With respect to synthesis, disclosed herein are three distinct synthetic strategies capable of producing diverse analogs bearing either a tricyclic cannabinol framework or a bicyclic scaffold inspired by cannabidiol: axially chiral cannabinols (axCBNs) or cannabidiols (axCBDs), respectively. Numerous products were obtained, including eight analogues which were examined for biological activity The initial structure-activity

relationship study revealed an *ax*Cannabinoid (*ax*CBN-3) with picomolar affinity for the hCB<sub>1</sub>R and hCB<sub>2</sub>R receptors as well as other promising leads (e.g., *ax*CBN-4 and *rac-ax*CBD-2) that display >5-fold selectivity for the hCB<sub>2</sub>R receptor over the hCB<sub>1</sub>R receptor. The *ax*Cannabinoids described here offer new opportunities to probe the binding sites of cannabinoid receptors and other protein targets of phytocannabinoids. Based on these findings, we plan to (1) further interrogate the biological activity and therapeutic potential of the initial lead molecules, and (2) utilize these findings to design and synthesize the next generation of *ax*Cannabinoids for drug discovery.

It is also worth noting that this strategy of converting point chirality into axial chirality can be applied *beyond* cannabinoids. Many bioactive natural products contain linked six-membered rings, and we speculate that scaffolds of this type have atropisomeric biaryl bioisosteres that may exhibit improved therapeutic, stability, and other ADMET properties (Figure 4). We propose that this type of structural modification be considered routinely throughout medicinal chemistry campaigns.

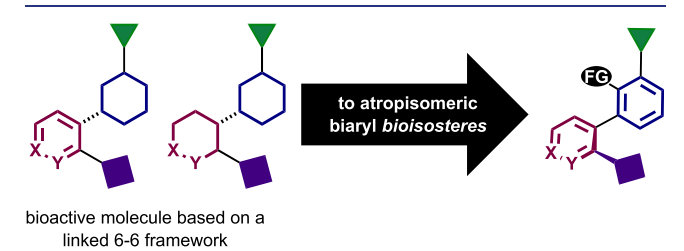


**Figure 4.** Beyond cannabinoids: other "lead molecules" in principle can have atropisomeric counterparts with potentially improved pharmaceutical/therapeutic properties.

#### ASSOCIATED CONTENT

# **5** Supporting Information

The Supporting Information is available free of charge at https://pubs.acs.org/doi/10.1021/jacs.3c00129.

Experimental procedures and characterization data (<sup>1</sup>H NMR, <sup>13</sup>C NMR, HRMS) (PDF)

### AUTHOR INFORMATION

# **Corresponding Authors**

Christopher W. Cunningham — Concordia University
Wisconsin School of Pharmacy, Mequon, Wisconsin 53097,
United States; orcid.org/0000-0002-4468-2213;
Email: chris.cunningham@cuw.edu

Thomas Gamage — Analytical Chemistry and Pharmaceutics, RTI International, Research Triangle Park, North Carolina 27709, United States; orcid.org/0000-0003-3528-9695; Email: tgamage@rti.org

Alexander J. Grenning — Department of Chemistry, University of Florida, Gainesville, Florida 32611, United States; orcid.org/0000-0002-8182-9464; Email: grenning@ufl.edu

#### Authors

Sara E. Kearney – Department of Chemistry, University of Florida, Gainesville, Florida 32611, United States

Anghelo J. Gangano – Department of Chemistry, University of Florida, Gainesville, Florida 32611, United States;
orcid.org/0000-0002-5577-5503

Daniel G. Barrus – Analytical Chemistry and Pharmaceutics, RTI International, Research Triangle Park, North Carolina 27709, United States

**Kyle J. Rehrauer** – Concordia University Wisconsin School of Pharmacy, Mequon, Wisconsin 53097, United States

Terry-Elinor R. Reid — Concordia University Wisconsin School of Pharmacy, Mequon, Wisconsin 53097, United States

Primali V. Navaratne – Department of Chemistry, University of Florida, Gainesville, Florida 32611, United States

Emily K. Tracy – Analytical Chemistry and Pharmaceutics, RTI International, Research Triangle Park, North Carolina 27709, United States

Adrian Roitberg — Department of Chemistry, University of Florida, Gainesville, Florida 32611, United States;
ocid.org/0000-0003-3963-8784

Ion Ghiviriga — Department of Chemistry, University of Florida, Gainesville, Florida 32611, United States; orcid.org/0000-0001-5812-5170

Complete contact information is available at: https://pubs.acs.org/10.1021/jacs.3c00129

# **Author Contributions**

The manuscript was written through contributions of all authors. All authors have given approval to the final version of the manuscript.

#### Notes

The authors declare the following competing financial interest(s): AJG and the University of Florida filed a provisional patent on chemical entities described in this manuscript.

#### ACKNOWLEDGMENTS

We gratefully acknowledge the National Institute of General Medical Science (R35 GM137893-01), the National Center for Complementary and Integrative Health (R01 AT010773), and the National Institute on Drug Abuse (K01 DA045752) for providing support for this research. This material is based upon work supported by the National Science Foundation (NSF CAREER 1844443). We thank the Mass Spectrometry Research and Education Center and their funding source: NIH S10 OD021758-01A1.

## REFERENCES

- (1) Bridgeman, M. B.; Abazia, D. T. Medicinal Cannabis: History, Pharmacology, and Implications for the Acute Care Setting. *P. T.* **2017**, *42*, 180–188.
- (2) Elikottil, J.; Gupta, P.; Gupta, K. The Analgesic Potential of Cannabinoids. J. Opioid Manag. 2009, 5, 341.
- (3) Scotter, E. L.; Abood, M. E.; Glass, M. The Endocannabinoid System as a Target for the Treatment of Neurodegenerative Disease. *Br. J. Pharmacol.* **2010**, *160*, 480.
- (4) Mechoulam, R.; Hanus, L. A Historical Overview of Chemical Research on Cannabinoids. *Chem. Phys. Lipids* **2000**, *108*, 1–13.
- (5) Ametovski, A.; Lupton, D. W. Enantioselective Total Synthesis of (-)-Δ9-Tetrahydrocannabinol via N-Heterocyclic Carbene Catalysis. *Org. Lett.* **2019**, *4*, 1212–1215.
- (6) Shultz, Z. P.; Lawrence, G. A.; Jacobson, J. M.; Cruz, E. J.; Leahy, J. W. Enantioselective Total Synthesis of Cannabinoids A Route for Analogue Development. *Org. Lett.* **2018**, *20*, 381–384.
- (7) Schafroth, M. A.; Zuccarello, G.; Krautwald, S.; Sarlah, D.; Carreira, E. M. Stereodivergent Total Synthesis of Δ9-Tetrahydrocannabinols. *Angew. Chem., Int. Ed.* **2014**, *53*, 13898–13901.
- (8) de Vries, M.; van Rijckevorsel, D. C.; Wilder-Smith, O. H.; van Goor, H. Dronabinol and Chronic Pain: Importance of Mechanistic Considerations. *Expert Opin. Pharmacother.* **2014**, *15*, 1525–1534.
- (9) Wissel, J.; Haydn, T.; Müller, J.; Brenneis, C.; Berger, T.; Poewe, W.; Schelosky, L. D. Low Dose Treatment with the Synthetic Cannabinoid Nabilone Significantly Reduces Spasticity-Related Pain: A Double-Blind Placebo-Controlled Cross-over Trial. *J. Neurol.* **2006**, 253, 1337–1341.
- (10) Nielsen, S.; Germanos, R.; Weier, M.; Pollard, J.; Degenhardt, L.; Hall, W.; Buckley, N.; Farrell, M. The Use of Cannabis and Cannabinoids in Treating Symptoms of Multiple Sclerosis: A Systematic Review of Reviews. *Curr. Neurol. Neurosci. Rep.* **2018**, *18*. 8.
- (11) Abu-Sawwa, R.; Scutt, B.; Park, Y. Emerging Use of Epidiolex (Cannabidiol) in Epilepsy. J. Pediatr. Pharmacol. Ther. **2020**, 25, 485–499
- (12) Beal, J. E.; Olson, R.; Laubenstein, L.; Morales, J. O.; Bellman, P.; Yangco, B.; Lefkowitz, L.; Plasse, T. F.; Shepard, K. V. Dronabinol as a Treatment for Anorexia Associated with Weight Loss in Patients with AIDS. *J. Pain Symptom Manage.* **1995**, *10*, 89–97.
- (13) Brafford May, M.; Glode, A. E. Cancer Management and Research Dovepress Dronabinol for Chemotherapy-Induced Nausea and Vomiting Unresponsive to Antiemetics. *Cancer Manage. Res.* **2016**, *8*, 49–55.
- (14) Devinsky, O.; Cross, J. H.; Laux, L.; Marsh, E.; Miller, I.; Nabbout, R.; Scheffer, I. E.; Thiele, E. A.; Wright, S. Trial of Cannabidiol for Drug-Resistant Seizures in the Dravet Syndrome. *N. Engl. J. Med.* **2017**, *376*, 2011–2020.
- (15) Adams, R.; Baker, B. R.; Wearn, R. B. Structure of Cannabinol. III. Synthesis of Cannabinol, 1-Hydroxy-3-n-Amyl-6,6,9-Trimethyl-6-Dibenzopyran 1. *J. Am. Chem. Soc.* **1940**, *62*, 2204–2207.
- (16) Bloemendal, V. R. L. J.; van Hest, J. C. M.; Rutjes, F. P. J. T. Synthetic Pathways to Tetrahydrocannabinol (THC): An Overview. *Org. Biomol. Chem.* **2020**, *18*, 3203–3215.

- (17) Maiocchi, A.; Barbieri, J.; Fasano, V.; Passarella, D. Stereoselective Synthetic Strategies to (–)-Cannabidiol. *ChemistrySelect* **2022**, 7, No. e202202400.
- (18) Dennis, D. G.; Anand, S. D.; Lopez, A. J.; Petrovčič, J.; Das, A.; Sarlah, D. Synthesis of the Cannabimovone and Cannabifuran Class of Minor Phytocannabinoids and Their Anti-Inflammatory Activity. *J. Org. Chem.* **2022**, *87*, 6075–6086.
- (19) Davis, M. P. Oral Nabilone Capsules in the Treatment of Chemotherapy-Induced Nausea and Vomiting and Pain. *Expert Opin. Invest. Drugs* **2008**, *17*, 85–95.
- (20) Burstein, S. H. Ajulemic Acid: Potential Treatment for Chronic Inflammation. *Pharmacol. Res. Perspect.* **2018**, *6*, No. e00394.
- (21) Tai, S.; Fantegrossi, W. E. Synthetic Cannabinoids: Pharmacology, Behavioral Effects, and Abuse Potential. *Curr. Addict. Rep.* **2014**, *1*, 129.
- (22) Brenneman, D. E.; Petkanas, D.; Kinney, W. A. Pharmacological Comparisons Between Cannabidiol and KLS-13019. *J. Mol. Neurosci.* **2018**, *66*, 121–134.
- (23) Liu, Y.; Ho, T. C.; Baradwan, M.; Pascual Lopez-Alberca, M.; Iliopoulos-Tsoutsouvas, C.; Nikas, S. P.; Makriyannis, A. Synthesis of Functionalized Cannabilactones. *Molecules* **2020**, *25*, 684.
- (24) Saldaña-Shumaker, S. L.; Grenning, A. J.; Cunningham, C. W. Modern Approaches to the Development of Synthetic Cannabinoid Receptor Probes. *Pharmacol. Biochem. Behav.* **2021**, 203, No. 173119.
- (25) Navaratne, P. V.; Wilkerson, J. L.; Ranasinghe, K. D.; Semenova, E.; Felix, J. S.; Ghiviriga, I.; Roitberg, A.; McMahon, L. R.; Grenning, A. J. Axially Chiral Cannabinols: A New Platform for Cannabinoid-Inspired Drug Discovery. *ChemMedChem* **2020**, *15*, 728–732
- (26) LaPlante, S. R.; Edwards, P. J.; Fader, L. D.; Jakalian, A.; Hucke, O. Revealing Atropisomer Axial Chirality in Drug Discovery. *ChemMedChem* **2011**, *6*, 505–513.
- (27) LaPlante, S. R.; Fader, L. D.; Fandrick, K. R.; Fandrick, D. R.; Hucke, O.; Kemper, R.; Miller, S. P. F.; Edwards, P. J. Assessing Atropisomer Axial Chirality in Drug Discovery and Development. *J. Med. Chem.* **2011**, *54*, 7005–7022.
- (28) Toenjes, S. T.; Gustafson, J. L. Atropisomerism in Medicinal Chemistry: Challenges and Opportunities. *Future Med. Chem.* **2018**, 409–422.
- (29) Wang, Z.; Meng, L.; Liu, X.; Zhang, L.; Yu, Z.; Wu, G. Recent Progress toward Developing Axial Chirality Bioactive Compounds. *Eur. J. Med. Chem.* **2022**, 243, No. 114700.
- (30) Basilaia, M.; Chen, M. H.; Secka, J.; Gustafson, J. L. Atropisomerism in the Pharmaceutically Relevant Realm. *Acc. Chem. Res.* **2022**, *55*, 2904–2919.
- (31) Brown, D. G.; Boström, J. Analysis of Past and Present Synthetic Methodologies on Medicinal Chemistry: Where Have All the New Reactions Gone? *J. Med. Chem.* **2016**, *59*, 4443–4458.
- (32) Yet, L. Biaryls. In *Privileged Structures in Drug Discovery*; Wiley, 2018; pp 83.
- (33) Munjal, M.; Elsohly, M. A.; Repka, M. A. Polymeric Systems for Amorphous Δ9-Tetrahydrocannabinol Produced by a Hot-Melt Method. Part II: Effect of Oxidation Mechanisms and Chemical Interactions on Stability. *J. Pharm. Sci.* **2006**, *95*, 2473–2485.
- (34) Huffman, B. J.; Shenvi, R. A. Natural Products in the "Marketplace": Interfacing Synthesis and Biology. *J. Am. Chem. Soc.* **2019**, *141*, 3332–3346.
- (35) Minuti, L.; Temperini, A.; Ballerini, E. High-Pressure-Promoted Diels-Alder Approach to Biaryls: Application to the Synthesis of the Cannabinols Family. *J. Org. Chem.* **2012**, *77*, 7923–7931.
- (36) Ashburn, B. O.; Carter, R. G. Diels—Alder Approach to Biaryls (DAB): Importance of the Ortho-Nitro Moiety in the [4 + 2] Cycloaddition. *Org. Biomol. Chem.* **2008**, *6*, 255–257.
- (37) Jin, S.; Niu, Y.; Liu, C.; Zhu, L.; Li, Y.; Cui, S.; Xiong, Z.; Cheng, M.; Lin, B.; Liu, Y. Gold(I)-Initiated Cycloisomerization/Diels-Alder/Retro-Diels-Alder Cascade Strategy to Biaryls. *J. Org. Chem.* **2017**, 82, 9066–9074.

- (38) Wilson, R. S.; May, E. L. Analgesic Properties of the Tetrahydrocannabinols, Their Metabolites, and Analogs. *J. Med. Chem.* **1975**, *18*, 700–703.
- (39) Schenherr, H.; Cernak, T. Profound Methyl Effects in Drug Discovery and a Call for New C H Methylation Reactions. *Angew. Chem., Int. Ed.* **2013**, 52, 12256–12267.
- (40) Godfrey, J. D.; Mueller, R. H.; Sedergran, T. C.; Soundararajan, N.; Colandrea, V. J. Improved Synthesis of Aryl 1,1-Dimethylpropargyl Ethers. *Tetrahedron Lett.* **1994**, *35*, 6405–6408.
- (41) Nicolaou, K. C.; Lister, T.; Denton, R. M.; Gelin, C. F. Total Synthesis of Artochamins F, H, I, and J through Cascade Reactions. *Tetrahedron* **2008**, *64*, 4736–4757.
- (42) Meepagala, K. M.; Estep, A. S.; Becnel, J. J. Larvicidal and Adulticidal Activity of Chroman and Chromene Analogues against Susceptible and Permethrin-Resistant Mosquito Strains. *J. Agric. Food Chem.* **2016**, *64*, 4914–4920.
- (43) Pearson, E. L.; Willis, A. C.; Sherburn, M. S.; Paddon-Row, M. N. Controlling Cis/Trans-Selectivity in Intramolecular Diels—Alder Reactions of Benzo-Tethered, Ester Linked 1,3,9-Decatrienes. *Org. Biomol. Chem.* **2008**, *6*, 513–522.
- (44) Gordo, J.; Avó, J.; Parola, A. J.; Lima, J. C.; Pereira, A.; Branco, P. S. Convenient Synthesis of 3-Vinyl and 3-Styryl Coumarins. *Org. Lett.* **2011**, *13*, 5112–5115.
- (45) Hlubucek, J.; Ritchie, E.; Taylor, W. C. Synthesis of 2,2-Dimethylchromenes. *Tetrahedron Lett.* **1969**, *10*, 1369–1370.
- (46) Wertjes, W. C.; Southgate, E. H.; Sarlah, D. Recent Advances in Chemical Dearomatization of Nonactivated Arenes. *Chem. Soc. Rev.* **2018**, *47*, 7996–8017.
- (47) Pottie, I. R.; Nandaluru, P. R.; Benoit, W. L.; Miller, D. O.; Dawe, L. N.; Bodwell, G. J. Synthesis of 6 H-Dibenzo[ b, d ]Pyran-6-Ones Using the Inverse Electron Demand Diels-Alder Reaction. *J. Org. Chem.* **2011**, *76*, 9015–9030.
- (48) Bonnesen, P. V.; Puckett, C. L.; Honeychuck, R. V.; Hersh, W. H. Catalysis of Diels-Alder Reactions by Low Oxidation State Transition-Metal Lewis Acids: Fact and Fiction. *J. Am. Chem. Soc.* 1989, 111, 6070–6081.
- (49) Murakami, M.; Itami, K.; Ito, Y. Directed Intermolecular [4 + 2] Cycloaddition of Unactivated 1,3-Diene Substrates with High Regio- and Stereoselectivities. *J. Am. Chem. Soc.* **1997**, *119*, 7163–7164.
- (50) Fürstner, A.; Stimson, C. C. Two Manifolds for Metal-Catalyzed Intramolecular Diels—Alder Reactions of Unactivated Alkynes. *Angew. Chem., Int Ed.* **2007**, *46*, 8845–8849.
- (51) Wender, P. A.; Smith, T. E. Transition Metal-Catalyzed Intramolecular [4+2] Cycloadditions: Mechanistic and Synthetic Investigations. *Tetrahedron* **1998**, *54*, 1255–1275.
- (52) Wender, P. A.; Jenkins, T. E. Nickel-Catalyzed Intramolecular [4 + 2] Dienyne Cycloadditions: An Efficient New Method for the Synthesis of Polycycles Containing Cyclohexa-1,4-Dienes. *J. Am. Chem. Soc.* **1989**, *111*, 6432–6434.
- (53) Jolly, R. S.; Luedtke, G.; Sheehan, D.; Livinghouse, T. Novel Cyclization Reactions on Transition-Metal Templates. The Catalysis of Intramolecular [4 + 2] Cycloadditions by Low Valent Rhodium Complexes. *J. Am. Chem. Soc.* **1990**, *112*, 4965–4966.
- (54) Gilbertson, S. R.; Hoge, G. S. Rhodium Catalyzed Intramolecular [4+2] Cycloisomerization Reactions. *Tetrahedron Lett.* **1998**, *39*, 2075–2078.
- (55) Saito, A.; Ono, T.; Takahashi, A.; Taguchi, T.; Hanzawa, Y. Rh(I)-Catalyzed Mild Intramolecular [4+2] Cycloaddition Reactions of Ester-Tethered Diene-Yne Compounds. *Tetrahedron Lett.* **2006**, *47*, 891–895.
- (56) Walker, D.; Hiebert, J. D. 2,3-Dichloro-5,6-Dicyanobenzoquinone and Its Reactions. *Chem. Rev.* **2002**, *67*, 153–195.
- (57) Kotha, S.; Chavan, A. S.; Goyal, D. Diversity-Oriented Approaches to Polycyclics and Bioinspired Molecules via the Diels-Alder Strategy: Green Chemistry, Synthetic Economy, and Beyond. *ACS Comb. Sci.* **2015**, *17*, 253–302.
- (58) Ashburn, B. O.; Carter, R. G.; Zakharov, L. N. Synthesis of Tetra-Ortho-Substituted, Phosphorus-Containing and Carbonyl-Con-

- taining Biaryls Utilizing a Diels-Alder Approach. J. Am. Chem. Soc. 2007, 129, 9109–9116.
- (59) Ashburn, B. O.; Carter, R. G. Diels—Alder Approach to Polysubstituted Biaryls: Rapid Entry to Tri- and Tetra-Ortho-Substituted Phosphorus-Containing Biaryls. *Angew. Chem., Int. Ed.* **2006**, *45*, 6737–6741.
- (60) Bow, E. W.; Rimoldi, J. M. The Structure–Function Relationships of Classical Cannabinoids: CB1/CB2 Modulation. *Perspect. Med. Chem.* **2016**, *8*, 17.
- (61) Rhee, M.-H.; Vogel, Z.; Barg, J.; Bayewitch, M.; Levy, R.; Hanuš, L.; Breuer, A.; Mechoulam, R. Cannabinol Derivatives: Binding to Cannabinoid Receptors and Inhibition of Adenylylcyclase. *J. Med. Chem.* 1997, 40, 3228–3233.
- (62) Friesner, R. A.; Murphy, R. B.; Repasky, M. P.; Frye, L. L.; Greenwood, J. R.; Halgren, T. A.; Sanschagrin, P. C.; Mainz, D. T. Extra Precision Glide: Docking and Scoring Incorporating a Model of Hydrophobic Enclosure for Protein–Ligand Complexes. *J. Med. Chem.* **2006**, 49, 6177–6196.